Presented at the 33rd European PV Solar Energy Conference and Exhibition, 25-29 September 2017, Amsterdam, The Netherlands

ULTRASONICALLY TINNED PVD AL REAR CONTACTS ON HIGH-EFFICIENCY CRYSTALLINE SILICON SOLAR CELLS FOR MODULE INTEGRATION

H. Nagel[1,*], D. Eberlein[1], S. Hoffmann[1], M. Graf[1], B. Steinhauser[1], F. Feldmann[1], A. Kraft[1], U. Eitner[1], M. Glatthaar[1], M. Hermle[1], S. W. Glunz[1], H. Haverkamp[2], T. Fischer[3], A. Hain[4], P. Wohlfart[4], V. Mertens, J. M. Müller[5] and T. Buck[6]

[1]Fraunhofer Institute for Solar Energy Systems (ISE), Heidenhofstraße 2, 79110 Freiburg, Germany
[2]Gebr. SCHMID GmbH, Robert-Bosch-Str. 32-36, 72250 Freudenstadt, Germany
[3]teamtechnik GmbH, Planckstraße 40, 71691 Freiberg, Germany
[4]SINGULUS TECHNOLOGIES AG, Hanauer Landstrasse 103, 63796 Kahl am Main, Germany
[5]Hanwha Q Cells GmbH, Sonnenallee 17-21, 06766 Bitterfeld-Wolfen, Germany
[6]International Solar Energy Research Center Konstanz e.V., Rudolf-Diesel-Straße 15, 78467 Konstanz, Germany
*Author for correspondence: Henning Nagel, Phone: +49 (0)761-4588-5493, e-mail: henning.nagel@ise.fraunhofer.de

ABSTRACT: We investigated ultrasonic tinning of physical vapor deposited (PVD) Al rear contacts on *p*-type passivated emitter and rear cells and *n*-type back junction cells, respectively. By means of electroluminescence (EL) imaging after ultrasonic tinning we identified small local damage of the cells' rear side passivation only at the positions where the soldering irons were initially placed on the Al. Though measured interconnector peel force was < 1 N/mm and hence lower then required by the standard DIN EN 50461, we obtained power degradation < 5 % after 400 thermal cycles, 2000 h in damp heat test and 20 cycles in the humidity freeze test, respectively, which is double the load demanded by the IEC 61215 standard. EL images revealed no local degradation induced by the climate tests. The microstructure of the tinned PVD Al is investigated by secondary electron microscopy and energy dispersive X-ray spectroscopy.
Keywords: metallization, back contact, module integration

1 INTRODUCTION

At present, most industrial-type crystalline silicon solar cells feature screen-printed rear contacts consisting of large-area Al and local Ag solder pads. However, the contacts suffer from shortcomings like possible reduction of the surface passivation of the cells due to the applied high sintering temperature, increased effective surface recombination velocity in comparison with boron back surface field (BSF) and damage of the *n*-doped BSF of *n*-type cells. Hence, high-efficiency c-Si solar cells often rely on physical vapor deposited (evaporated or sputtered, PVD) Al. It makes good ohmic contact to *p*- and *n*-type Si, provides excellent back reflection of infrared light passing through the cells and features very high electrical conductivity. However, for a broad industrial utilization of PVD Al, a reliable interconnection technology is needed. In this work, we studied local ultrasonic tinning of PVD Al, a technology that was originally developed for screen-printed Al [1, 2]. To the best of our knowledge, the application to PVD Al was not comprehensively reported before.

2 EXPERIMENTAL

Two types of 6 inch CZ Si solar cells were investigated: about 21 % efficient *n*-type back junction cells prepared by Hanwha Q Cells [3] and about 20 % efficient *p*-type front junction passivated emitter and rear cells (PERC) featuring locally laser-fired PVD Al rear contacts on top of an electrically passivating Al_2O_3/SiN stack. The Al on the rear of the PERC cells was deposited in a high-rate inline thermal evaporation vacuum system to a thickness of about 2.7 µm. The front sides of both cell types were contacted by screen-printed and fired Ag. In order to make the rear Al solderable, 3 tin busbars were simultaneously applied within 6 s per cell by ultrasonic soldering irons in a setup equipped with automated cell transport, see Figure 1. 99.9 wt% pure Sn was used without flux. During tinning, the cells were positioned on a temperature controlled chuck at 270 °C. Sn wires were fed to the tips of the irons which were heated to 380 °C. In an automated tabber-stringer 1.5 mm x 0.2 mm Cu ribbons with standard SnPb coating were soldered onto the cells by means of controlled infrared lamp heating. Because Cu interconnectors and Al were already tinned, we obtained very good solder wetting. Subsequently, the cells were interconnected to 3-cell-strings. Two strings, one of every cell type, were laminated in each of the 3 manufactured photovoltaic modules. The cross-sectional construction of the modules was soda-lime glass / ethylene vinyl acetate (EVA) / solar cells / EVA / Tedlar-PET-Tedlar backsheet. Illuminated *IV* curves of the individual strings in the modules were measured at standard test conditions (25 °C, 1000 W/m², AM1.5G). Electroluminescence (EL) images were taken under forward bias. The *IV* and EL measurements were performed before and after light-induced degradation (3 h under 1 sun halogen-lamp illumination) and after subsequent damp heat, thermal cycling and humidity

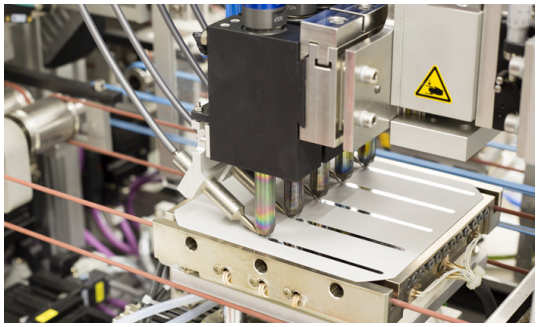

Figure 1: Photo of the ultrasonic tinning process applied to the Al rear contact on a CZ Si solar cell. Departing from this photo, the cells in the study featured 3 busbars instead of 5.

freeze tests according to the standard IEC 61215. On individual strings, which were not laminated into modules, the 90° peel force of interconnectors soldered onto the back side was measured. In order to investigate the microstructure and composition of tinned PVD Al on the rear of PERC cells, cross sections were prepared by ion milling and studied by secondary electron microscopy (SEM) as well as energy dispersive X-ray spectroscopy (EDX).

For the purpose of demonstrating the efficiency potential, a 'TopCon' solar cell [4] featuring a full-area carrier-selective contact on the back side and PVD Al as a metal electrode on the rear *n*-doped Si layer was prepared. The cell was characterized by illuminated *IV* measurement.

3 RESULTS AND DISCUSSION

3.1 Microstructure of the tinned PVD Al rear contact

We investigated the microstructure of the tinned PVD Al in order to shed light on potential failure mechanisms in case of mechanical stress. Our analysis was confined to *p*-type PERC cells. The SEM images depicted in Figure 2 show cross sections of the ultrasonically tinned PVD Al on the alkaline textured rear of the cells. After tinning, the cells were annealed with the same temperature profile as used for the soldering of interconnectors. It can be seen from the upper picture, that Al and Sn resemble the textured Si surface well without large gaps. However, a conspicuous result is that there are small voids in the Sn bulk featuring diameters of about 100 nm. We explain their formation by the well known cavitation effect: When liquids – in this case molten Sn – are subjected to ultrasound the sonic waves locally create low pressure that ruptures the liquid. During cool down the Sn solidifies fast and the formed cavities are frozen into it. The voids are also present at the interface between Sn and Al as can be seen in the middle picture. Because their number per unit area is small at the interface, we expect that the voids don't reduce the adherence of Sn on the PVD Al significantly.

On the microscale the Sn most often is also in intimate contact to the PVD Al, see SEM picture in the middle. However, in some areas very narrow gaps are located between Sn and Al. Obviously Sn didn't wet Al well there during ultrasonic soldering. Since the area of these spots is notable, it can be concluded that non-wetting plays a role when it comes to the mechanical adherence of the Sn layers to the Al.

After applying mechanical force, the Sn layer was detached from the Al as can be seen in the lower picture. Because we didn't observe fracture in the Sn, Al or Si bulk at any studied position, the Sn-Al interface appears to be the weakest site. This is confirmed by the interconnector pull-off tests described below.

EDX mappings of tinned PVD Al cross sections are shown in Figure 3. It can be seen from the upper picture that no extended intermetallic phases at the interface between Sn and Al are formed. This is known from the alloy phase diagram [5]. In general, it can be expected that this limits the adherence of Sn on Al. The lower picture in Figure 3 reveals a disrupted Al_2O_3 layer at the same interface which is the intended consequence of

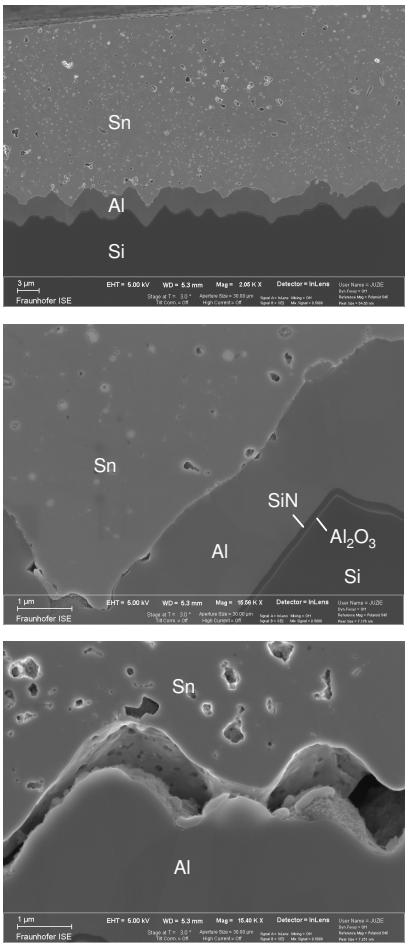

Figure 2: SEM pictures showing three cross sections of ultrasonically tinned PVD Al on the alkaline textured rear of *p*-type PERC cells.

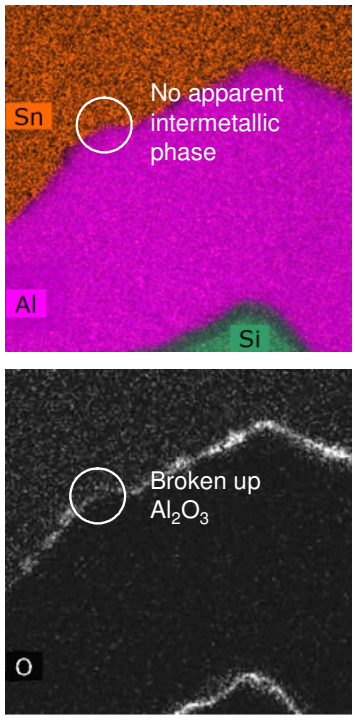

Figure 3: EDX cross-sectional view of an ultrasonically tinned PVD Al rear contact on a *p*-type PERC cell. Image width: 5.8 µm.

applying ultrasound during tinning. In some areas the Al_2O_3 seems to be still intact, but no gap between Sn and Al is visible at this position.

Note that at the bottom edge in the lower picture of Figure 3 an about 10 nm thick Al_2O_3 surface passivation layer can be seen.

3.2 Interconnector peel force

The normalised 90° interconnector peel force measured on *p*-type PERC cells after stringing is shown in Figure 4. It is 0.5 N/mm on an average. This value does not comply with the standard DIN EN 50461 (> 1 N/mm). The failing interface was between the Sn deposited by ultrasonic soldering and the PVD Al in accordance with the findings described in paragraph 3.1. We expect that the adherence can be increased e. g. by increasing the ultrasonic power during Al tinning.

Apparently, the adherence of PVD Al on the dielectric passivation layer stack is higher. It must be mentioned that it is a strong function of the top dielectric layer material. Recently, in a work on 'PassDop' solar cells we found that the adherence of thermally evaporated Al is very high on SiO_2 and very low on MgF_2 [6]. In [7] we reported high adherence of thermally evaporated Al on SiN and very high adherence on crystalline Si. Furthermore, the adherence of PVD Al on dielectric layers depends on the thermal treatment before Al deposition [8] and the substrate temperature during Al deposition, see [9].

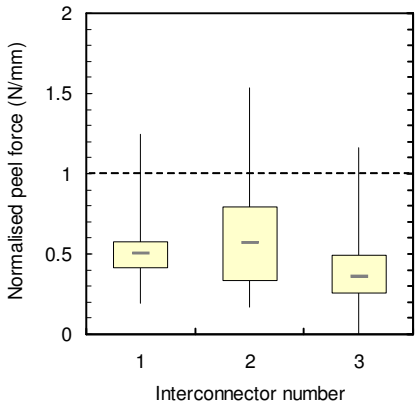

Figure 4: Measured normalised 90° peel force of interconnectors soldered on ultrasonically tinned PVD Al rear contacts of *p*-type PERC cells.

3.3 Module climate tests

Figure 5 shows the electrical power at maximum power point (P_{mpp}), the open-circuit voltage (V_{oc}), the short-circuit current density (J_{sc}) and the fill factor (*FF*) of the prepared 3-cell-strings in photovoltaic modules measured under standard test conditions. The values were normalised to the ones before light-induced degradation (LID). The strings contain the *p*-type front-junction laser-fired contact PERC cells (upper graph) and *n*-type rear-junction cells (lower graph), respectively. The measurement sequence depicted from left to right in each graph is a) illuminated *IV* measurement before LID, b) after LID (3 h under 1 sun halogen-lamp illumination), c) after 200 thermal cycles from -40 °C to 80 °C and d) after 400 thermal cycles. Power degradation is below 5 % (dotted horizontal line) and hence meets the standard IEC 61215. Note that we performed twice the number of cycles required. It is also worth to mention that in Figure 5 V_{oc} of both cell types increased after 200 and 400 cycles compared with the initial state. Obviously, defects in the bulk and/or at the surfaces were annealed during the elevated module test temperature.

Figure 6 depicts EL images taken from the *p*-type PERC strings in the thermal cycling test. The pictures reveal that the upper two cells in the string suffer from LID. The reason is the formation of BO-complexes in the

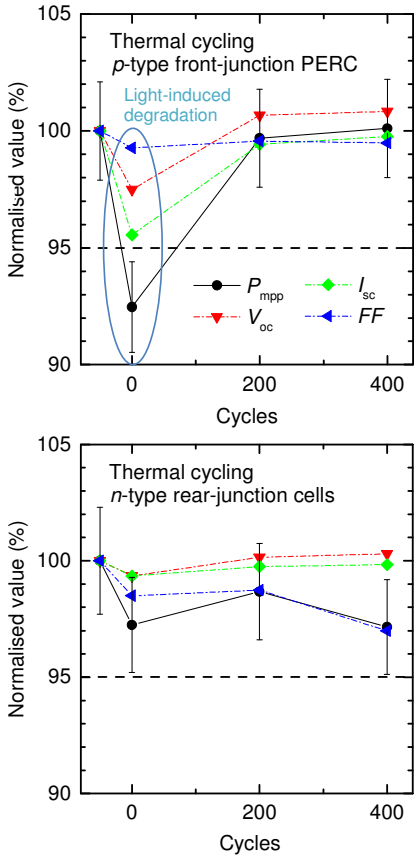

Figure 5: Measured electrical performance parameters of 3-cell-strings laminated in photovoltaic modules measured before and after LID and after subsequent thermal cycles between -40 °C and 85 °C.

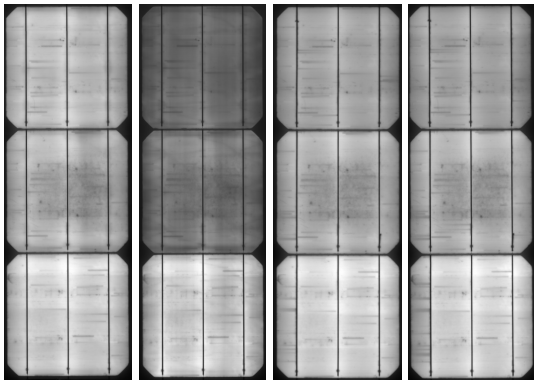

Figure 6: EL images of the 3-cell-string investigated in the upper graph in Figure 5. The pictures were taken under forward bias after consecutive LID and thermal cycling stress.

CZ Si bulk under illumination. Subsequently, during elevated temperatures in the thermal cycling test BO-complexes dissociate and both cells recover.

The EL images after 200 and 400 cycles virtually are the same as before LID. Hence, excellent stability against the applied stress is proven on the whole cell surfaces.

Figure 7 shows the corresponding EL images of the *n*-type rear-junction cells. Again, there is no visible local degradation after thermal cycling. Additionally, the *n*-type Si cells don't suffer from LID as expected.

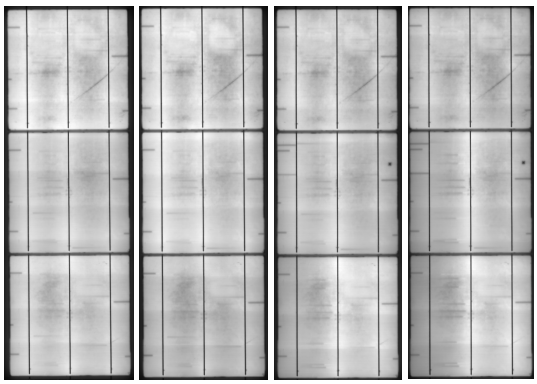

Figure 7: Forward bias EL images of the 3-cell-string investigated in the lower graph in Figure 5. The pictures were taken after consecutive LID and thermal cycling stress.

A close look at the electroluminescence images in Figures 6 and 7 reveal that the cells' rear side electrical passivation is not damaged by ultrasonic tinning of the capping PVD Al layer except where the soldering iron first came in touch with the Al. Optimization of the tinning process e. g. by lowering the ultrasound power at the beginning of the tin busbars can probably eliminate the damage there.

Figures 8 and 9 show the normalised electrical performance parameters of 3-cell-modules measured before and after LID and after subsequent damp heat test (85 °C and 85 % relative humidity) and humidity freeze test (-40 °C to 85 °C at 85 % relative humidity). Again, highest power degradation was 4 % after double IEC 61215 testing. The EL images of the strings (not shown here) revealed no visible local degradation due to the climate tests.

3.4 High-efficiency TopCon cell

Table 1 shows the measured electrical performance parameters of a 10 x 10 cm² large TopCon cell featuring a 1 µm thick PVD Al rear contact. An efficiency of 23.4 % was obtained. From the high open-circuit voltage of 713 mV and electroluminescence imaging (not shown here) we deduce that the PVD Al did not spike through the *n*-doped Si layer on the rear of the cell. However, the cell's series resistance is above what was expected due to

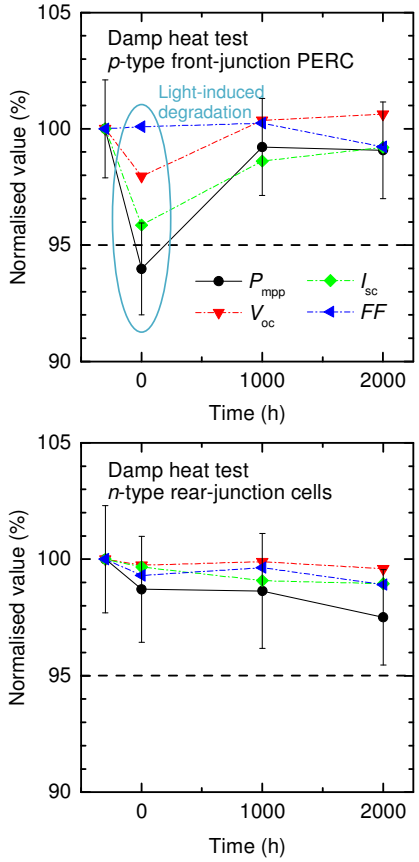

Figure 8: Measured electrical performance parameters of 3-cell-strings laminated in photovoltaic modules measured before and after LID and after subsequent damp heat test.

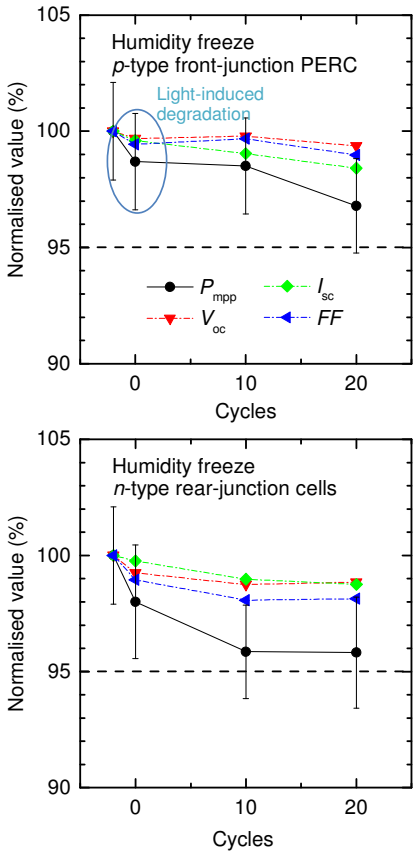

Figure 9: Measured electrical performance parameters of 3-cell-strings in modules before and after LID and after humidity-freeze cycles. Upper picture: *p*-type front junction PERC cells. Lower picture: *n*-type rear-junction cells.

a high contact resistance of about 150 mΩ cm² between Al and *n*-doped Si as measured on extra test samples. Hence, further process optimization is needed.

Note that the thermally evaporated PVD Al adheres well on the *n*-doped Si. Hence, it was possible to ultrasonically tin the Al as described before for the *p*-type PERC and the *n*-type rear-junction cells.

Table 1: Measured illuminated *IV* parameters of a 100 cm² TopCon solar cell featuring PVD Al rear metal contact.

V_{oc} (mV)	J_{sc} (mA/cm²)	*FF* (%)	Eta (%)	R_{ser} (mΩ cm²)
713	40.3	81.5	23.4	0.59

4 SUMMARY AND CONCLUSION

Ultrasonic tinning of PVD Al was investigated for making the rear contact of high-efficiency Si solar cells solderable. Electroluminescence imaging revealed that the cells' rear electrical passivation was not damaged by ultrasonic tinning of the capping PVD Al except at very small positions where the soldering iron first came in touch with the Al. The measured average normalised 90° interconnector peel force after stringing was 0.5 N/mm on *p*-type PERC cells which does not yet comply with the standard DIN EN 50461 (> 1 N/mm). The failing interface was between ultrasonically deposited Sn and PVD Al.

A high stability of the prepared modules in the performed climate tests was found. After double thermal cycling, damp-heat and humidity freeze tests the electrical power degradation was below 5 %. No local degradation became obvious from EL images.

In order to demonstrate the performance of PVD Al as a rear contact, a 100 cm² TopCon cell was prepared reaching an efficiency of 23.4 %. The contact resistivity of the PVD Al on the *n*-doped Si layer limited the fill factor.

In conclusion, ultrasonically tinned PVD Al rear contacts are a reliable solution for manufacturing solderable high-efficiency Si solar cells. Ultrasonic tinning of PVD Al can easily be implemented at the end of the cell processing sequence and is characterized by a high technology readiness level. In order to increase the interconnector peel force, further optimization e. g. of the ultrasonic power is necessary.

ACKNOWLEDGEMENT

The authors thank the German Federal Ministry for Economic Affairs and Energy for funding within the projects 'IdeAl' under contract number 0325889B.

5 REFERENCES

[1] H. v. Campe, S. Huber, S. Meyer, S. Reiff and J. Vietor, Proceedings of the 27th European Photovoltaic Solar Energy Conference, p. 1150, 2012.

[2] P. Schmitt, D. Eberlein, C. Ebert, M. Tranitz, U. Eitner and Harry Wirth, Energy Procedia 38 (2013) p. 380.

[3] V. Mertens, T. Ballmann, J. Cieslak, M. Kauert, A. Mohr, F. Stenzel, M. Junghänel, K. Suva, Ch. Klenke, G. Zimmermann and J. W. Müller, Proceedings of the 28th European Photovoltaic Solar Energy Conference, p. 714, 2013.

[4] F. Feldmann, B. Steinhauser, S. Kluska, M. Hermle and S. W. Glunz, this conference.

[5] A. J. McAlister and D. J. Kahan, Bulletin of Alloy Phase Diagrams 4 (1983) 410.

[6] B. Steinhauser, A. Büchler, H. Nagel, S. Kluska, J. Benick, P. Saint-Cast, S. Gutscher, J. Bartsch and Martin Hermle, Energy Procedia (2017) in press.

[7] H. Nagel, M. Kamp, D. Eberlein, A. Kraft, J. Bartsch, M. Glatthaar and S. W. Glunz, Proceedings of the 32nd European Photovoltaic Solar Energy Conference, p. 48, 2016.

[8] J. Kumm, P. Hartmann, D. Eberlein and A. Wolf, Thin Solid Films 612 (2016) p. 393.

[9] J.R. Black, 15th Int. Reliab. Phys. Symp. Las Vegas, p. 257, 1977.